Top Med Chem (2020) 34: 149–184
DOI: 10.1007/7355_2019_90

Published online: 11 March 2020

Applications of Fluorescent Protein-Based Sensors in Bioimaging

Uday Kumar Sukumar, Arutselvan Natarajan, Tarik F. Massoud, and Ramasamy Paulmurugan

Contents

Abstract In the last two decades, there have been enormous developments in the area of reporter gene imaging for various bioimaging applications, especially to track cellular events that are occurring in intact cells and cells within living animals. As part of this process, there has been a significant interest in identifying new reporters or developing new substrates that can allow us to image multiple cellular events simultaneously without any signal overlap between the targets. Even though chemical dyes are useful for some of these applications, reporter proteins which mimic biological properties of proteins when tagged directly with the target proteins are very useful. Although molecular imaging has significantly advanced through use of different imaging probes (radiolabeled ligands, MR contrast agents, CT contrast agents, fluorescent dyes, fluorescent and bioluminescent proteins) and techniques (PET, SPECT, MRI, CT, optical, ultrasound, and photoacoustic imaging), optical imaging, such as fluorescence and bioluminescence imaging, has shown promising applications in various preclinical settings, especially in imaging cellular pathways and studies involving drug development. This is mainly owing to its simple and easy

U. K. Sukumar, A. Natarajan, T. F. Massoud, and R. Paulmurugan (✉)
Molecular Imaging Program at Stanford, Department of Radiology, Stanford University School of Medicine, Stanford, CA, USA
e-mail: paulmur8@stanford.edu

nature in performing the assay and also its high-throughput and cost-effective applications. In this chapter, we review the evolution of optical imaging with specific emphasis on fluorescent proteins, as well as an introduction regarding the general approach of optical imaging in in vitro and in vivo applications. We explain this by briefly introducing different optical imaging methods and fluorescent assays developed based on fluorescent dyes and fluorescent proteins followed by a detailed review of different fluorescent proteins currently used for various assay developments and applications.

Keywords BRET, Fluorescence dyes, Fluorescent proteins, FRET, In vivo imaging

1 Introduction

Fluorescent proteins and fluorescent dyes are routinely used to monitor biological processes of cells in culture or cells in living animals; hence they are called fluorescent reporters (FR). This includes fluorescent proteins, organic dyes, and inorganic photonic materials. Fluorescent reporters are commonly used for developing assays involving fluorescence spectroscopy, fluorescence microscopy, and whole-body preclinical imaging and to some extent in human applications for image-guided surgery in the operating room [1, 2]. Fluorescent reporters in combination with an optical imaging system can provide key information in clinical oncologic research while providing the opportunity to develop transgenic animal models for studying various diseases, including cancer. Fluorescent dyes are widely used in various bioassay applications. Here, we mainly discuss the role of fluorescent protein as reporters (FPR) in various sensor designs and applications in bioimaging, drug delivery, and drug discovery systems. We also briefly discuss the role of fluorescent dyes in imaging applications (Fig. 1).

2 Fluorescent Biosensors and Evolution of Fluorescent Protein Palette

Fluorescent proteins are frequently used for studying molecular mechanisms of cells and physiological processes involved in cellular biological pathways. A plethora of fluorescent proteins with characteristic excitation and emission spectra offer enormous scope for researchers to "paint" living cells as they desire [3]. At present we have gone a step further and created sophisticated biosensors engineered with single or multiple fluorescent proteins, including Förster Resonance Energy Transfer (FRET)-based biosensors for studying macromolecular interactions in cells [4]. These fluorescent proteins exhibit environment-dependent changes in fluorescent

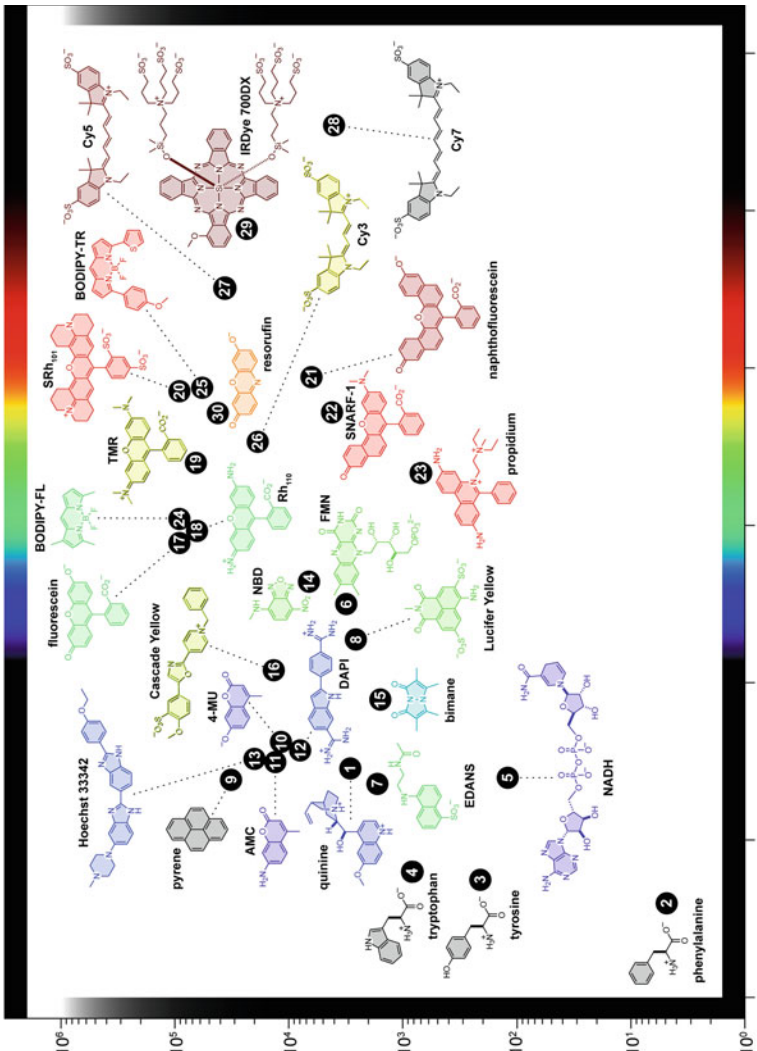

Fig. 1 Fluorescent dyes of various spectral properties developed in the last several decades and used for bioimaging applications in preclinical and clinical studies Adapted with permission from ACS Chem. Biol., 2008, 3(3), pp. 142–155 [2]

spectral characteristics and act as biosensors (1) to measure target enzyme functions (e.g., protein kinases and proteases); (2) to measure the concentration of intracellular ions, metabolites, and messengers (H^+, Ca^{2+}, Cl^-, H_2O_2, cAMP, etc.); (3) to monitor cellular physicochemical parameters (i.e. specific analyte, covalent modification, mechanical influence, redox potential, membrane potential); and (4) for high-throughput screening of drug candidates and their evaluations in preclinical studies. One of the earliest fluorescent proteins to be discovered was green fluorescent protein (GFP), when, in 1962, a Japanese organic chemist and marine biologist Osamu Shimomura stumbled upon this remarkable protein in the jellyfish *Aequorea victoria* [5]. At present this discovery has reached beyond the realm of science and our homes with the development of transgenic fluorescent fishes and green fluorescent pigs and cats [6, 7]. The first use of GFP as a fluorescent tag for in vivo labeling was demonstrated in 1995 by Dhandayuthapani et al., where they reported the application of GFP-engineered mycobacteria (*M. smegmatis* and *M. bovis* BCG) for analysis of fundamental biological and pathogenesis related to mycobacteria [8]. It was rather serendipitous that GFP turned out to be a natural monomer which enabled its wide use for labeling of various proteins of interest by simple in-frame fusion to the –COOH or $–NH_2$ terminus or even as an insert within a flexible loop of a protein [9].

Biosensing encompasses a diverse array of techniques for the generation of an experimentally accessible "readout" of a molecular interaction between a biomolecule-derived molecular recognition element (MRE) (e.g., a protein domain) and an analyte of interest (e.g., a small molecule, another protein, or an enzymatic activity) [10, 11]. Molecular entities or devices that enable biosensing are generally referred to as biosensors. The primary challenge of creating biosensors is transducing the nanometer-scale event of a biorecognition process into an observable change in a macroscopic property such as color or fluorescence hue [12]. One of the nanometer-scale changes that typically accompany biorecognition events is the change in molecular "geometry" of the MRE. This change could be a distance between the MRE and its analyte, as in the case of a protein-protein interaction, or a conformational change of the MRE, as in the case of allosteric proteins [13–15]. As we will discuss in this chapter, researchers have now devised a variety of strategies to develop fluorescent protein-based biosensors for many applications [16].

The protein-based fluorescent biosensors can be broadly categorized into two classes based on the construction method: the first class are genetically encoded fluorescent proteins such as GFP and its variants, whereas the second class comprises of chemically constructed biosensors made of natural protein scaffolds and artificial fluorescent molecules [17]. We will primarily discuss protein-based fluorescent biosensors in this chapter. In the case of genetically encoded biosensors (GFP-based), the GFP protein acts as a signal transducer that manifests change in fluorescence intensity or wavelength shift in response to triggered stimuli. Different versions of such biosensors have been established in the past, including single FP-based biosensors, split GFP-based biosensors, and dual FP-fused FRET-based biosensors [18]. Such biosensors are a powerful tool for in-cell imaging and/or elucidating biological events of cells in normal and pathological processes.

With the rapid progresses being made in exploring diverse applications of fluorescent proteins in biosensors, one of the major considerations is improving the "brightness" of the fluorophore to achieve higher sensitivity. The brightness of fluorescent protein depends on how well a molecule absorbs light and how fast it emits light. Light absorption by a fluorophore is quantified in terms of molecular extinction coefficient, whereas emission of light intensity is quantified by quantum yield. A promising fluorescent protein for designing a biosensor is identified based on the high quantum yield of the protein. The quantum yield relates the efficiency at which a fluorescent molecule converts absorbed photons into emitted photons, i.e., number of photons emitted divided by the number of photons absorbed, with an efficiency of 1.0 being the maximum possible value. Since it is difficult to know the precise number of photons absorbed without specialized instrumentation, the typical practice of measuring quantum yield depends on comparing the unknown to a known standard [19, 20]. In most of the fluorescent proteins, the quantum yield of the fluorophore is not solely determined by absorbed photons but also by other environmental factors such as pH, temperature, polarity, etc.

The construction of fluorescent biosensors generally relies on the rational design of the strategy, which begins with an effort to find a macromolecular receptor with appropriate affinity and specificity to the target. The second step integrates the receptor molecular recognition event into suitable fluorescent signal transduction, which involves foreign reporter moieties such as an engineered autofluorescent protein (AFP). The resultant possibilities for the engineered biosensor are then screened based on biosensor quantum yield, sensitivity, and measurement dynamics [21]. In spite of a seemingly simple procedure, researchers are attempting to fabricate a novel fluorescent biosensor for a given target that would inevitably struggle with unexpected labor intensity in screening such large possibilities of random mutagenesis. The field of computational biology and machine learning offers an exceptional brute force approach in screening the such large sea of variants, by placing a "virtual" molecule of interest in the binding site of a virtual receptor [22]. The program sequentially mutates the receptor amino acids involved in binding the ligand, searching for sequences that form a surface complementary to the ligand. Typically, even with 12–18 amino acids mutations, around 10^{23} variants arise which excludes the possibility of in vitro screening. Finding productive biosensors with high quantum yield and sensitivity in such a large number of possibilities requires powerful computational algorithms. The success of such algorithms depends on how precisely the model recapitulates the energy (or "fitness") of the interacting groups. However, when approaching this problem computationally, not only the amino acid sequence of the receptor must be specified but also the orientation of the ligand, as well as the various conformations that might be adopted by the side chains of the mutated amino acids. Different models have evolved over the course of time for protein biosensor engineering, for instance, Rangefinder, a computational algorithm developed by Mitchell et al., which performs in-silico screening of dye attachment sites in a ligand-binding protein for the conjugation of a dye molecule to act as a Förster acceptor for a fused fluorescent protein [23]. Such computational protein designs have been successfully used to precisely arrive at efficient protein models; a

few to highlight here include a hyperthermophilic protein [24], two small molecule biosensor proteins [25], two novel enzymes [26, 27], and a novel protein fold [28]. Thus, computational in-silico approach holds great promise in future for designing and optimization of biosensors. While developing mutants for designing biosensors, it is also important to consider the use of infrared and near-infrared (NIR) fluorescent proteins as a choice for enhancing the in vivo imaging capability of the developed biosensors.

Green fluorescent protein (native state) is a 21 kDa protein consisting of 238 amino acid residues forming a secondary structure of 5 α-helices and 1 11-stranded β-pleated sheet, where each strand contains 9–13 amino acid residues each [29]. Substitution of specific amino acids has generated a wide range of GFP variants with distinct spectral characteristics. For instance, substituting Tyr66 for His, Trp, or Phe results in blue-shifted spectral variants. Extensive mutagenesis of *Aequorea victoria* GFP has produced a series of monomeric FPs of a variety of colors: blue [30, 31], violet [32], cyan [30, 31, 33, 34], green [35–37], and yellow [38]. This palette enables multicolor labeling of proteins of interests and FRET-based techniques. Breakthrough in the red fluorescent protein field occurred only after the discovery of DsRed and other red fluorescent and chromoproteins from Anthozoa species [39–41]. These discoveries opened the way for the development of orange, red, and far-red FPs with emission peaks located as far as 655 nm [42]. However, the vast majority of natural FPs and chromoproteins cloned from various species during the past 10 years are tetramers, such as FPs from anthozoa [39–41] and copepods [43, 44], or dimers, such as anm2CP and phiYFP from hydrozoa [44].

3 Genetically Encoded Sensors (GES)

The genetically encoded fluorescent proteins have opened new avenues for developing biosensors to visualize and quantify activity or conformational state of proteins of interest, especially changes in the concentration of molecular and physiological events in cells, tissues, or whole organism [45]. The intercellular/intracellular signaling pathways, cell communications, differentiation, and development have been investigated extensively with these fluorescent proteins [46]. One of the promising applications include in vivo imaging of individual neurons in transgenic animals with calcium-responsive genetically encoded biosensors [47]. At the intracellular levels, genetically encoded biosensors can be used to spatiotemporally decipher the complex network of interactions that occur between proteins, nucleic acids, and other macromolecules (Fig. 2) [48]. The chemically synthesized sensitive fluorescent dyes differ greatly from fluorescent proteins in terms of their relevance, sensitivity, specificity, development, and applications. The genetically encoded fluorescent protein sensors are introduced into the host cells as genetic materials by either transient transfection or knock-in techniques which allows cellular endogenous biogenesis pathways to express these as proteins [49]. Such an intricate integration with endogenous biogenesis eliminates the possibility of unintended

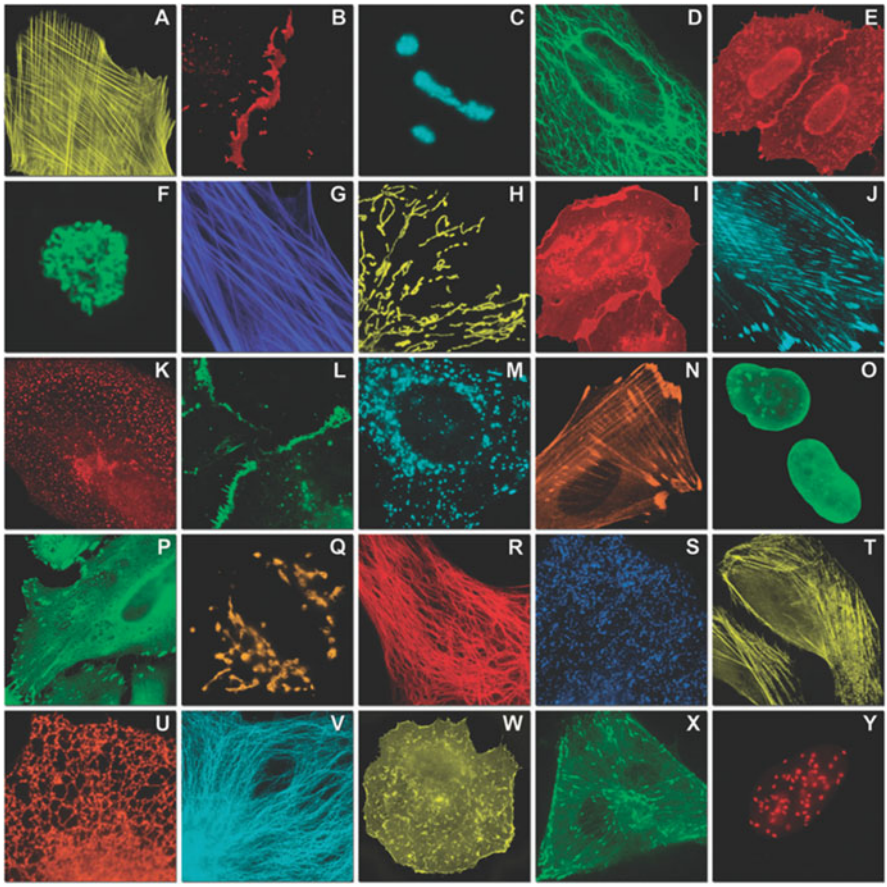

Fig. 2 Different fluorescent protein constructs with specific subcellular localization; FP-fusion partner: (**a**) mOrange2-b-actin, (**b**) mApple-Cx43, (**c**) mTFP1-fibrillarin, (**d**) mWasabi-cytokeratin, (**e**) mRuby-annexin (A4), (**f**) mEGFP-H2B, (**g**) EBFP2-b-actin, (**h**) mTagRFP-T-mitochondria, (**i**) mCherry-C-Src, (**j**) mCerulean-paxillin, (**k**) mKate-clathrin (light chain), (**l**) mCitrine-VE-cadherin, (**m**) TagCFP-lysosomes, (**n**) TagRFP, (**o**) superfolderGFP-lamin, (**p**) EGFP-a-v-integrin, (**q**) tdTomato-Golgi, (**r**) mStrawberry-vimentin, (**s**) TagBFP-Rab, (**t**) mKO2-LC-myosin, (**u**) DsRed2-endoplasmic reticulum, (**v**) ECFP-a-tubulin, (**w**) tdTurboRFP-farnesyl, (**x**) mEmerald, (**y**) mPlum-CENP-B. Adapted with permission from Richard et al., with copyrights [48]

perturbation in endogenous pathways by the biosensor itself while probing target; thus, they allow fluorescence imaging with a closer representation to the in vivo system over a longer period of time [50]. On the other hand, fluorescent dyes are limited by their stability, photobleaching, and cytotoxicity, which are often driven by their non-native interaction with biomolecules that interferes with endogenous fate of the analytes, and thus might limit relevance of such a study to single time point analysis alone [51]. Furthermore, unlike dyes, GES are not prone to leakage during long-term experiments and offer high-throughput screening in drug development.

GES, by virtue of being derived from naturally evolved proteins or protein components of cells, open the possibility for targeting them virtually to any compartment or microcompartment of cells through fusion with an appropriate domain or by introducing short terminal peptides to form appropriate signal motifs [58–60]. The design of fluorescent biosensors is based on a rationale of introducing a nimble manipulation of target domains or fluorescent proteins, which involves conformational changes in the spectral properties of fused domains or distance change, dipole orientation shift between two proteins capable of FRET. FRET is a physical phenomenon in which a donor fluorophore upon excitation transfers the energy non-radiatively to a neighboring acceptor fluorophore, thereby causing the acceptor to emit its characteristic fluorescence of longer wavelength range [18]. Since FRET is highly sensitive to the distance between donor and acceptor dipoles within the 1–10 nm range, they have become a valuable tool to deduce biochemical events involving changes in molecular proximity, such as protein-protein interactions, conformational changes in proteins, intracellular ion concentrations, and enzyme activities [61].

The genetically encoded fluorescent sensors can be broadly categorized into four groups according to the basic principles of the designs (Fig. 3):

1. Intrinsic environment sensitive fluorescent protein biosensor (single FP-based sensors)
2. Engineered single FP-based sensors
   (a) Incorporating a conformationally sensitive detector domain
   (b) Circularly permuted FP sensors
3. FRET-based sensors containing two FPs
4. Translocation sensors/assays

Each of these sensor categories has distinct applications owing to their characteristics. Single native fluorescent proteins are the preferred option for ion sensors, whereas engineered fluorescent proteins and two protein systems are better options for deducing structural changes or a protein-protein FRET interaction, respectively.

3.1 Intrinsic Environment-Sensitive Fluorescent Protein Biosensor (Single FP-Based Sensors)

As an intrinsic property of GFP and its derivatives, the spectral properties of the chromophores are determined by the environment (i.e., pH or conformational change). This property has been exploited to develop biosensors that measure pH [53, 62, 63], halide anions [64], and redox potentials [65, 66]. The environment-induced change within the chromophore pocket of fluorescent protein offers flexibility for generating variation in the fluorescence spectrum to probe analyte-specific signal.

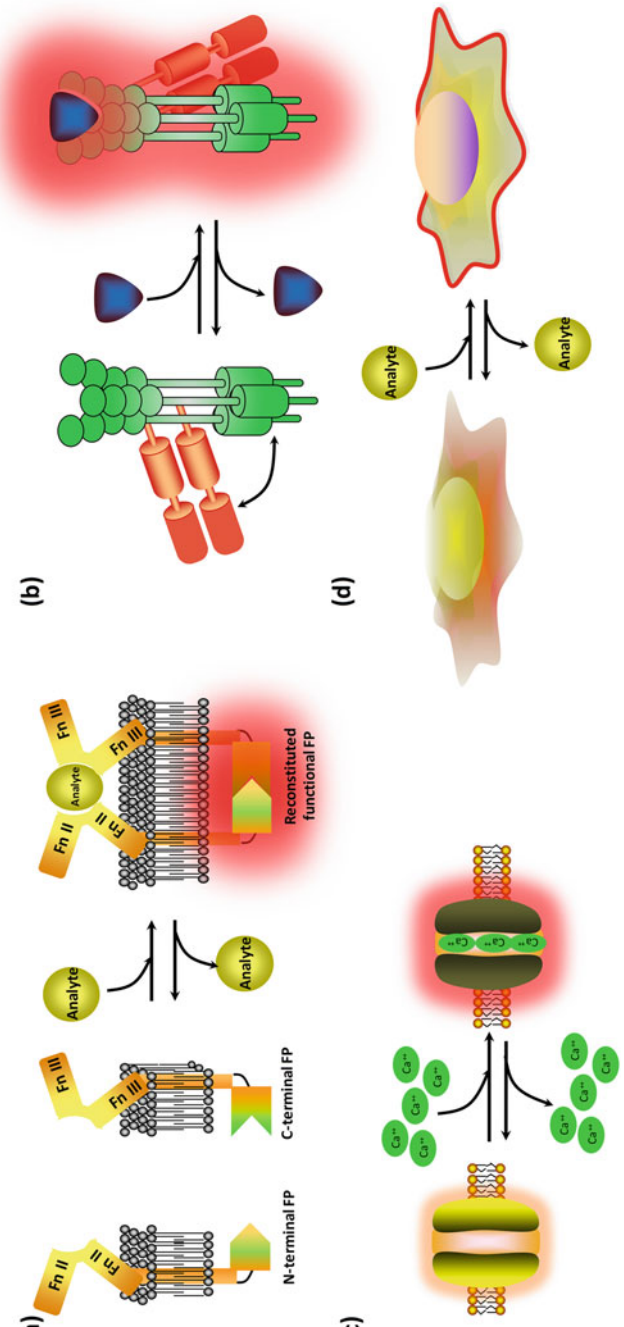

Fig. 3 Different types of FP-based fluorescent sensors: (**a**) circularly permuted FP fused to specific sensitive domain(s). (**b**) Two FPs of different colors are fused to sensitive domain(s); those conformational changes influence the efficiency of FRET between these FPs. (**c**) Intrinsically sensitive FP undergoes ion-dependent changes in spectral properties (brightness or excitation-emission wavelengths), e.g., pH. (**d**) Translocation sensors: FP fused to specific protein domains demonstrates environmentally dependent changes in intracellular localization

3.1.1 Fluorescent Biosensors as Tool for Detection of Intracellular Ion Concentrations

The pH-responsive fluorescent proteins have been used to monitor exocytosis and recycling of proteins based on the rationale of prevalent acidic pH of the secretory vesicles [52, 67] (Table 1). The chromophores of most of the fluorescent proteins naturally possess sensitivity to pH, specifically those carrying GFP-like or DsRed-like chromophores, which indicates that any FP can be used as a sensor to monitor pH changes in living cells [53, 68]. Especially in proteins with GFP-like chromophores, the proportion of charged ground-state chromophores (with excitation peak at ~480 nm) grows with increase in pH, up to pH 9.0, whereas the proportion of protonated chromophores (with excitation at ~400 nm) declines. This property explains the observed increase in fluorescence of green or yellow fluorescent protein with increase in pH upon excitation at 480–500 nm. The shift in fluorescence intensity in pH is rapid and reversible (<1 ms) [63]. Overall, the pH sensitivity of fluorescent sensors is determined by the p*K*a of the charged chromophore, which in turn determines the pH value at which the intensity of green fluorescence begins to decline by 50% of I_{max}, and the Hill coefficient determined by slope of fluorescence versus pH at a given p*K*a point. Fluorescent proteins with p*K*a of ~6.0 are suitable to measure pH changes in acidic compartments, while some of the less acid-tolerant yellow FPs can be used to measure pH changes in the cytosol [67]. Fluorescent proteins with different p*K*a values are generated by rational modification of core amino acids in the chromophore pocket or by random mutagenesis. A pH-sensitive mutant variant called super-ecliptic pHluorin manifests ~50-fold increase in fluorescence in response to change in pH from 5.5 to 7.5 and has been used for monitoring synaptic vesicle cycling at nerve terminals [69]. Another such variant of monomeric red FP, mKeima, exhibits a large Stokes shift with respect to change in pH. Depending upon the neutral (protonated) and anionic (deprotonated) state of chromophore, it exhibits bimodal excitation spectra with peaks at 438 and 550 nm, with a single emission peak at 620 nm [70, 71]. The chromophore has p*K*a of 6.5, and the pH acts as a ratiometric pH sensor based on the ratio of ionized state at a given pH. Another crucial factor in determining the implication of such fluorescent sensors for pH sensing is also based on their stability in different pH range. In this

Table 1 Genetically encoded fluorescent sensors – single fluorescent protein (FP) sensors

Analyte	Sensor name	Components	Sensor type	Reference
pH	SynaptopHluorin	pHluorin	pH-sensitive green FP	[52]
pH	mNect.hCNT3	mNectarine	pH-sensitive red FP	[53]
Ca^{2+}	GCaMP3	M13-cpGFP-calmodulin	Single cpFP	[54]
Ca^{2+}	Case12	M13-cpGFP-calmodulin	Single cpFP	[55]
Ca^{2+}	Camgaroo-2	Calmodulin domain into YFP	Peptide insertion	[56]
H_2O_2	HyPer	OxyR	Single cpFP	[57]

aspect, mKeima exhibits high resistance to lysosomal enzyme-mediated degradation; this inspired and resulted in the modification of mKeima as an autophagy sensor, specifically to detect the event of conversion of autophagosomes to autolysosomes. In the fluorescent pH sensor, mKeima was fused with light chain 3 (LC3) of microtubule-associated protein [72]. Under starvation-induced autophagy, LC3 is cleaved and allows recruitment of phosphatidylethanolamine to the outer and inner membranes of autophagosome, which then fuses with the lysosomes leading to the degradation of packaged cargo under a highly acidic environment [73]. The mKeima-LC3 probe enabled visualization of these autolysosomal maturation events by detection of the acidification-induced color change of mKeima and provided a cumulative fluorescent readout of autophagic activity, with the deduction of the hallmark event of autophagy, i.e., LC3 localization. Another variant of mKeima, pH-Red, was developed with a specific purpose of achieving pH-dependent readout in near-infrared region. This property can provide the advantage of light emission with higher penetration and less light scattering in biological tissues and thus offer advantage for deep tissue pH monitoring across a broad pH range. pHRed with an apparent pKa of 6.6 demonstrated nearly tenfold change in ratio of fluorescence emission upon excitation with a wavelength of 585 nm [74].

To date, various GES for monitoring pH have been generated in such as way they can respond with either changes in fluorescent brightness of a single fluorescence peak or ratiometric changes with two excitation peaks [75]. The latter type of pH sensors imply ratiometric measurement of fluorescence brightness excited at two different wavelengths and hence are free from artifacts that arise owing to variable protein concentrations, cell thickness associated signal attenuation, cell movement, or excitation intensity since measurement in one peak can normalize the other peak that was used for pH measurement [75]. Ratiometric pH sensors commonly respond with a change in the ratio of excitation efficiency at 400 nm versus 480 nm owing to a shift in the protonated/deprotonated chromophore ratio [52]. An internal control of overall signal stability can be the intensity of fluorescence excitation at the isosbestic point between the two excitation peaks, at ~430 nm. Another type of ratiometric GES that utilizes the pH-sensitive efficiency of excited state proton transfer (ESPT) from the protonated GFP chromophore excited at 400 nm. These sensors are excited at 400 nm and respond with a change of fluorescence ratio between 450 nm and 510 nm [62]. Ratiometric pH sensors can also be developed by fusing pH-stable and pH-sensitive fluorescent protein variants of different colors. In this case, changes in the fluorescence brightness ratio of the two fused FPs can be measured along with FRET efficiency between the two FPs, as discussed in detail below.

Fluorescent protein-based sensors for measuring metal ions in living cells can be categorized into intensiometric sensors which change in fluorescence intensity when the chromophore bound to a metal ion and ratiometric biosensors that exhibit shift in the absorption or emission spectra when the chromophore bound to a metal ion. The intensiometric fluorescent sensors are the preferred option for developing quantitative assays, since their fluorescence intensity has been determined by the sensor concentration in each cell and the path length in addition to the ion concentration.

Ratiometric biosensors are severely limited for quantitative estimations owing to their lower sensitivity (i.e., smaller dynamic range), larger spectral bandwidth, and the need to acquire images with two combinations of excitation and emission filters for fluorescence measurement.

The sensitivity of biosensor for measuring ionic concentration has been determined by its binding affinity for an ion and its dynamic range. Binding affinity of an ion can be defined in terms of dissociation constant (Kd), which is the ion concentration at which 50% of the sensor binding sites are occupied. This can be experimentally determined by sensor titration experiments. Dynamic range is essentially an indicator of a sensor's measurement sensitivity and its signal-to-noise ratio (SNR). In order to monitor ion concentration changes, it is preferable to choose a sensor that is 20% saturated at baseline, whereas a sensor that is ~50% saturated at baseline is more suitable for comparing differences in resting ion concentrations in different cells or different environmental conditions. For instance, Cameleon-Nano sensors have lower Kd and are better for quantitative measurement of cytosolic Ca^{2+} in some cell types, whereas D1ER is preferred for ER measurement because Ca^{2+} levels are high in the ER and the Kd of D1ER is much higher than other Cameleons. Tables 2 and 3 summarize Kd and DRs of some ratiometric ion sensors which are designed for measuring ion concentrations in subcellular organelles.

3.2 Fluorescent Protein Complementation (Split Fluorescent Proteins) Sensors

3.2.1 Sensors Fused with Intermediate Recognition Domains from Target Proteins for Designing the Biosensors

To expand the scope of sensors specific to some analytes, an analyte-specific extrinsic recognition domain has been inserted into FPs. In the conventional design of bimolecular fluorescent complementation (BiFC) sensors, a FP is split into two fragments and then fused to recognition domains that are associated with the analytes of interest [86, 87]. The two halves of the FP do not emit fluorescence in the state of dissociation since no intact chromophore will be reconstituted. Upon the analyte-induced change in the recognition domains, the complementary fragments of the FP are brought into close proximity and reconstitute the β-barrel chromophore structure of the FP, resulting in the recovery of the fluorescence signal. In general, split FP strategies have a much lower background so that it may produce a greater dynamic range than those of FRET and single FP-based biosensors. On the other hand, a major drawback of split FP-based biosensors is that they are not reversible. While irreversibility provides a significant advantage for detecting transient and/or weak interactions, it is not suitable for analyzing dynamics of an analyte in real time [88]. Study of protein-protein interaction involves split FP fragments that do not associate with each other spontaneously. In this strategy, the fluorescent protein halves are fused to two different target proteins of interest. In the event of interaction

Table 2 Ratiometric biosensors for imaging Ca^{2+} and Zn^{2+} ions

Ratiometric Ca^{2+} biosensors						
Fluorescent proteins used	Sensors name	Ca^{2+}-responsive elements	Kd′ for Ca^{2+}	Hill coeff.	Comments	Reference
Yellow Cameleon series	YC2.60	CaM, M13p	93.5 nM	2.7	Not available	[76]
Yellow Cameleon series	YC3.60	CaM E104Q, M13p	215 nM, 779 nM	3.6, 1.2	High dynamic range	[77]
Yellow Cameleon Nano series	YC-Nano50	CaM, M13p	52.5 nM	2.5	Optimized for detecting subtle cytosolic Ca^{2+} in living organisms	[76]
D-family Cameleons	D1	mCaM, mM13p	0.8 μM, 60 μM	1.18, 1.67	Does not bind endogenous CaM; optimized for ER	[78]
D-family Cameleons	D3	cpV mCaM, mM13p	0.6 μM	0.74	Does not bind to endogenous CaM; optimized for cytosol and mitochondria	[79]
Troponin C family	TN-XXL	mTpC	800 nM	1.5	Optimized for imaging of neurons; fast response	[80]
Ratiometric Zn^{2+} biosensors						
Fluorescent proteins used	Sensors name	Zn^{2+}-responsive elements	Kd′ for Zn^{2+}	Hill coeff.	Comments	Reference
Zap family	ZapCY1	Zap	2.53 pM	1	Optimized for ER, Golgi, and mitochondria; high dynamic range	[81]
ZinCh family	eZinCh	CFP and YFP	8.2 μM	1	Targeted to vesicles by fusion to VAMP2	[82]
eCALWY family	eCALWY4	Atox1 and the WD4 domain of ATP7B	630 pM	1	Optimized for cytosol	[81]
Zap family	ZapCY2	mZap	811 pM	0.44	Optimized for cytosol	[83]

between target proteins, the split FP halves are brought together, resulting in assembly of functional fluorescent protein with intact chromophore which results in the appearance of fluorescence. This approach provides straightforward interpretation for extent and location of target protein interaction in the cell. A drawback of BiFC as compared to FRET sensors is that upon reassociation of split FP fragments,

Table 3 Sensors targeted to subcellular locations

Subcellular location	Ca^{2+} sensors	Zn^{2+} sensors	Reference
Golgi	None	Golgi-ZapCY1	[83]
ER	D1ER	ER-ZapCY1	[78, 83]
Vesicles	Ycam2	eZinCh	[81, 84]
Mitochondria	4mt-D3cpV	Mito-ZapCY1	[79]
Nucleus	D3cpV	ZapCY2	[83, 85]
Cytosol	D3cpV	eCALWY-4, ZapCY2	[81, 83, 85]

it takes from minutes to hours for the chromophore to mature and produce fluorescent signal, which limits their applications in real-time detection of protein-protein interactions [86]. Apart from this, the split FP assembly is irreversible in most cases, although there have been reports of partial recovery of split FP [89]. On the other hand, the BiFC system achieves higher sensitivity and detects even weak interactions as it accumulates signal over time, thus prevailing over FRET sensors in this aspect [90]. Numerous variants of split fluorescent protein-based sensors with different spectral properties have emerged over the years, e.g., blue (EBFP), cyan (ECFP, Cerulean, SCFP3A), green (EGFP), and yellow (EYFP, Venus, Citrine) mutants of *Aequorea victoria* GFP [91–94]. In addition split variants of red and far-red FPs such as mRFP1 [94], mCherry [95], DsRed-monomer [96], and mKate [97] have their origin from other fluorescent proteins. As a result of common origin from same FP, fragments from different color mutants with complementary fragments also yield cross-associated species with distinct spectral properties, which extends the application of these systems in competitive protein binding interactions [92, 98]. The other possibility of using two split FPs of different origins capable of hybrid formation may be applied to visualization of two independent pairs of protein-protein interactions [95, 96]. The combination of cross-associated BiFC and non-cross-associated BiFC system enables simultaneous detection of three pairs of protein-protein interactions taking place within the same cells at any given time point [97].

In the cases of certain BiFC, chimeric proteins consisting of fragments from different proteins sometimes reconstitute chromophore and emit fluorescence, which offers diverse fluorescent shades capable of tracking multiple events simultaneously in cells [96]. As an example of such a multicolor BiFC chimera, the event of ligand-dependent oligomerization (homodimer and heterodimer) between adenosine A 2A and dopamine D2 receptors was evaluated effectively in a differentiated neuronal cell model [99].

Another emerging strategy is based on incorporation of unnatural amino acids (UAAs) into a natural chromophore of fluorescent protein for developing single FP sensors. The incorporation UAA to proteins has recently emerged as a strategy to generate novel rationally engineered single FP sensors [100]. One of the earliest reports on this approach was made by Yun and coworkers wherein GFP-dopa mutant was generated by replacing all tyrosine residues in the GFP with metal-chelating L-DOPA [101]. The mutant variant functioned as a selective Cu^{2+} sensor. Similarly

another group introduced a metal-binding amino acid, HqAla (2-amino-3-(8-hydroxyquinolin-5-yl)propanoic acid), into the Tyr66 of a cpsfGFP variant that enabled this construct to achieve a 7.2-fold increase in fluorescence intensity in the presence of Zn^{2+} ions in living *E. coli* cells [102]. Apart from affinity-based unnatural amino acids, chemically reactive UAAs also serve as an option for reaction-based fluorescent protein biosensors. Schultz and coworkers exploited this approach in designing an FP sensor (UFP-Tyr66pBoPhe) for detection of H_2O_2 by substituting Tyr66 of GFP with *p*-borono-L-phenylalanine (pBoPhe) carrying an H_2O_2-reactive arylboronate side chain [102]. In the absence of H_2O_2, the chromophore remains electron deficient owing to the presence of electron withdrawing vacant 2p orbital of boron, and as a result of which, the sensor does not produce fluorescence. However, in the presence of H_2O_2, pBoPhe is oxidized to the original tyrosine residue, leading to quick recovery of fluorescence [103]. Although initially UAA-based sensors were speculated to behave unsuccessfully in in vivo systems owing to the synthetic origin of UAA, a few recent reports have achieved the same in mammalian cells. An UAA-based H_2S sensor was developed by substitution of Tyr66 with *p*-azido-L-phenylalanine (pAzF) and was successfully expressed in mammalian cells and illustrated as response time of mere ~7 min upon addition of 50 μM of NaHS [104]. The azide-modified chromophore in the presence of H_2S is selectively reduced which results in the observed fluorescence enhancement. The same group also developed genetically encoded mammalian cells compatible for peroxynitrite probe on the basis of the similar strategy [105].

The oligomeric aspect of fluorescent proteins offers flexibility for designing dimerization-dependent fluorescent sensors that also enables reversible fluorescence change upon complementation [106]. For instance, the oligomeric Discosoma red FP (DsRed) and the RFP heterodimer (ddRFP-A1B1) exhibit weak fluorescence in the monomeric state but upon heterodimerization manifest tenfold higher fluorescence with a Kd of 33 μM. A series of red intensiometric biosensors based on a diverse color palette ddRFP, ddGFP, and ddYFP have been created for detection of PPIs, Ca^{2+} dynamics, and protease activity with improved brightness and contrast [107]. The efficient SNR of the system enabled imaging of endomembrane proximity between endoplasmic reticulum and mitochondria clearly distinguishable.

3.2.2 Biosensors Designed Using Circularly Permuted FPs

The close proximity of N- and C-termini observed in many three-dimensional protein structures has been used in the past to perform circular permutation experiments on many different proteins [108]. The circularly permuted FP (cpFP)-based GES are quite promising owing to the potentially high dynamic range of fluorescence spectral shifts. A circular permutation is a relationship between proteins whereby they have a changed order of amino acids in their peptide sequence resulting in a reconstituted protein with overall similar 3D shape but with different N- and C-termini [109]. In the case of cpFP-based sensors, conformational changes of sensory domains yield structural changes in the chromophore environment and

thus strongly influence change in the spectral properties of the cpFPs. The influence is usually brought by factors such as protonation/deprotonation of a GFP-like chromophore, as well as changes in its fluorescence quantum yield and molar extinction coefficient. A rationally engineered cpGFP offers robust variants which sustains fluorescence emission even after insertion of peptides or proteins to the new terminus. The predominant permuted variants as per GFP sequence arise from a permutation point in the vicinity of amino acid positions [62, 66]. The proximity of sensitive fusion domains to the chromophore pocket in the fluorescent protein determines extent of influence on the native spectral properties. In the case of cpECFP, cpEGFP, and cpEYFP, insertion of calmodulin (Ca^{2+}-binding protein) in a specific position localized it in close proximity to the chromophore in the folded 3D conformation, which resulted in deprotonation of the chromophore and subsequent shift in fluorescence emission [60, 110]. As a follow-up to this pioneering study, several groups developed single cpFP-based biosensors with different binding domains for the detection of calcium [54, 111, 112], cGMP [113], H_2O_2 [57], and Zn(II) [114].

In cpFPs, the recognition domain in the presence of an analyte can undergo a conformational change by itself as well as influence conformational change in the fused fluorescent protein that is reflected by change in the fluorescence spectra. One example of this approach is a G-CaMP sensor for Ca^{2+}, which has a calmodulin (Ca^{2+}-binding protein) fused to the C-termini of a cpEGFP and a M13 peptide (a synthetic peptide with calmodulin-binding domain) fused to the N termini [115]. The success of the G-CaMP biosensor design inspired further modification for improving the sensitivity while developing a diverse range of color palettes for multicolor imaging of Ca^{2+} level in different organelles of cells, such as cytosol, nucleus, and mitochondria, at single-cell level [116].

The routine approach of permutation in FPs involves fusion of sensitive domains close to the chromophore in order to manifest a change in its spectral properties [77, 117]. With this strategy, numerous calcium sensors [55, 112, 118, 119] and hydrogen peroxide sensors [57], phosphorylation sensors [120], and membrane potential sensors [121, 122] have emerged successfully in the recent past. Incorporation of binding protein with competitive analyte affinity can serve as a new type of ratiometric sensor. Incorporation of adenylate binding protein GlnK1 with differential affinity for ATP and ADP into cpYFP could generate sensors with different spectral properties depending upon the analyte ADP or ATP [123].

Hydrogen peroxide is an important signaling molecule, and a sensor specific for detection of hydrogen peroxidase, i.e., HyPer, was designed based on yellow cpFP incorporated into the H_2O_2-sensitive OxyR regulatory domain [124]. The sensor detects submicromolar concentration of H_2O_2 by selective oxidation of OxyR residues and leads to change in yellow cpFP chromophore environment with corresponding ratiometric change in fluorescence excitation spectrum, i.e., fluorescence ratio upon excitation at 420 nm with respect to excitation at 500 nm. The sensor was later successfully modified for the detection of wounds using zebra fish as a model organism [125].

3.3 FRET Sensors

The phenomenon of Förster or Fluorescence Resonance Energy Transfer (FRET) was first described by Theodor Förster in 1946 [126]. In principle FRET is a physical phenomenon in which a donor fluorophore in its excited state non-radiatively transfers its excitation energy to a neighboring acceptor fluorophore which is located in close proximity, thereby causing the acceptor to emit its characteristic fluorescence. As FRET involves non-radiative transfer of energy, it is highly sensitive to the distance between donor and acceptor dipoles within the 1–10 nm range [127]. Thus, FRET has found extensive application as a spectroscopic ruler in monitoring molecular interactions, because the distances that can be measured are much shorter than the diffraction limit of conventional microscopy and even super resolution microscopy. In case of fluorescent protein-based FRET sensors, the donor and the acceptor are fluorescent proteins with distinct spectral properties. The two proteins upon interaction undergo conformational change and alter the proximity of chromophores and its orientation, which promotes the occurrence of FRET [128]. The efficiency of FRET is inversely proportional to the sixth power of distance within the short range of 10 nm [129]. The inverse sixth power law relation leads to detectable change in energy transfer even for change in orientation/proximity at the molecular scale between the interacting chromophores. Such small-scale molecular interactions include protein-protein interactions, conformational changes, intracellular ion concentrations, and enzyme activities (Fig. 4).

The efficiency of FRET (i.e., the quantum yield of the energy transfer) between any two FPs is determined by the overlap of the emission spectrum of the donor and the excitation spectrum of acceptor, quantum yield of donor fluorescence, and extinction coefficient of the acceptor. A 30% or higher overlap in the emission spectra of donor and excitation spectra of acceptor is a prerequisite for achieving sufficient FRET signal with a reliable detection limit. Apart from this, the proximity of the donor and acceptor governs the FRET efficiency by inverse power law. The quantum yield and extinction coefficient of fluorophores determine the sensitivity and yield of FRET signal. For any given pair of chromophores involved in FRET, an integral factor representing the abovesaid parameters is denoted by the Förster distance (R_0), which is the distance at which the FRET efficiency is 50% of its maximal value.

With the advent of a wide range of GFP variants with distinct excitation and emission spectra, the possibility of donor/acceptor combination has increased dramatically. Initial FRET-based biosensors were predominantly based on BFP as energy donor, which was hampered by its instability and lower brightness. Recently, cyan fluorescent protein (CFP) and donor yellow fluorescent protein (YFP) have become the most useful FRET pairs for many in vitro studies. Following this trend, two novel FRET pairs (mAmetrine/tdTomato and mCitrine/mTFP1) were developed for simultaneous imaging of two different enzymes in a single-cell level.

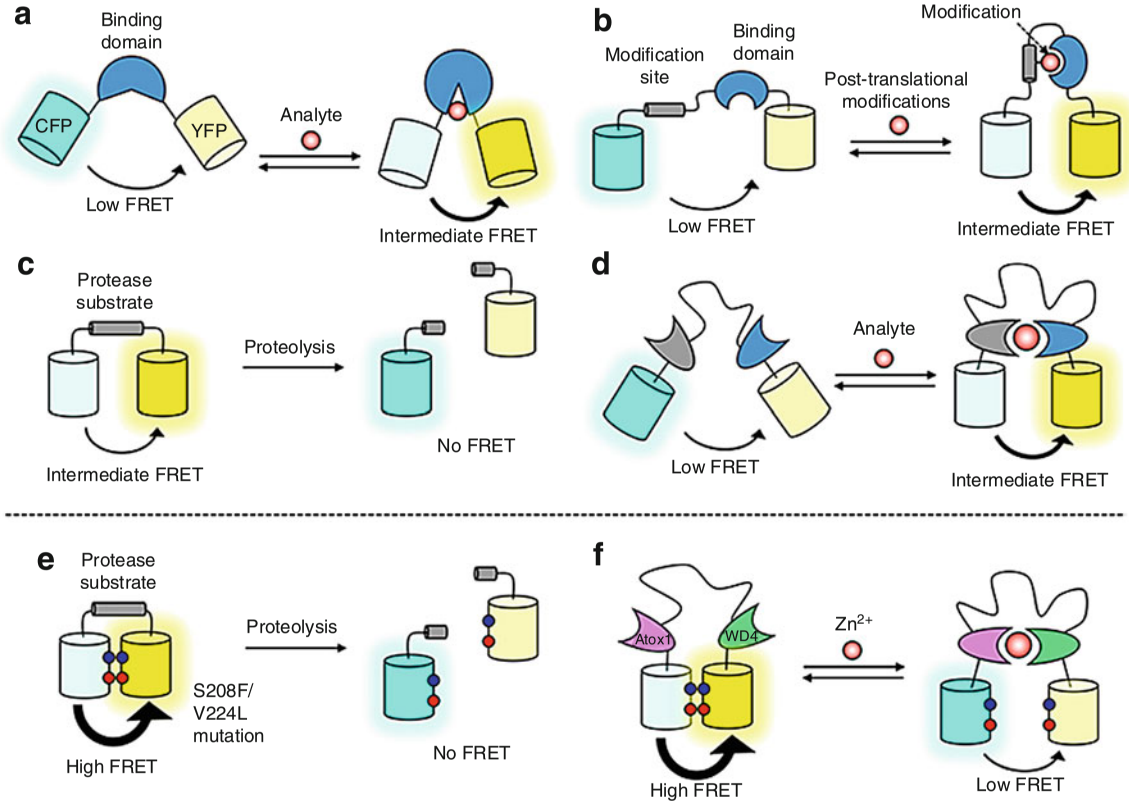

Fig. 4 Representative design formats for FRET-based biosensor: (**a**) a single binding domain undergoes a conformational change upon binding analyte. (**b**) Biosensors to monitor posttranslational modifications. (**c**) Biosensors to detect protease activity. (**d**) Biosensors based on an analyte-dependent protein-protein interaction. (**e**, **f**) FRET-based sensors based on self-associating FPs. (**e**) Protease sensor. (**f**) eCALWY sensor for Zn^{2+}. Adapted from Tamura et al., with copyrights [128]

Table 4 FRET-based fluorescent protein sensors

Sensor type	Sensor name	Components	Principle of work	Reference
cGMP	cGES-DE5	YFP-GKI-B-CFP	Structural rearrangement of domain	[130]
Ca^{2+}	TN-XXL	CFP-2x (COOH-terminal lobe of troponin C)-cpYFP	Structural rearrangement of domain	[80]
Ca^{2+}	Yellow Cameleon3.6	ECFP-calmodulin-M13-cpVenus	Interaction of domains	[77]
Ca^{2+}	Cameleon D3	ECFP-calmodulin-M13-cpVenus (redesigned calmodulin and M13)	Interaction of domains	[79, 131]
Caspase-3 activity	CaspeR3	TagGFP-DEVD-TagRFP	Cleavage of the linker	[132]
PKA activity	AKAR1	ECFP-14-3-3-substrate-YFP	Interaction of domains	[133]
Membrane potential	Mermaid	Ci-VSP-mUKG-mKOk	Structural rearrangements near membrane	[134]
Membrane potential	VSFP2.4	Ci-VSP-YFP-mKate2	Structural rearrangements near membrane	[135]

3.3.1 Types of FRET Biosensors

The intramolecular FRET probes/sensors involve two fluorescently tagged proteins that bring them into close proximity in the event of an interaction between the two analytes to generate FRET signal. In the following section, we also classify FRET biosensors by their way of transforming a biological change into a change in FRET efficiency. A brief list of such FRET-based biosensors is summarized in Table 4.

3.3.2 Cleavage-Based FRET Biosensors

The cleavage-based FRET biosensors are the most prevalent sensors because of their versatility in design and application. The constituent FRET pair is linked by a short cleavable peptide sequence that in its uncleaved state shows FRET signal owing to the proximity of the donor and acceptor, whereas in the presence of a linker peptide as a specific enzyme, cleavable substrate leads to dissociation of two fluorophores and loss of FRET signal upon cleavage. This signal is evident as a shift in acceptor emission to donor emission. One of the major drawbacks of such FRET systems as compared to other counterparts is the irreversibility of the sensors because they are driven by irreversible cleavage of linker peptides; this limits their ability to sense target analytes to only one event. Therefore, they find application mostly to

Table 5 Cleavage-based FRET biosensors

Target	Type	FRET pair	Reference
Caspase-3	Apoptosis	CFP, YFP	[136]
Caspase-3 and caspase-6	Apoptosis	CFP, YFP, mRFP	[137]
Caspase-3 and caspase-8	Apoptosis	CFP, YFP	[138]
Caspase-3 and caspase-8	Apoptosis	seCFP, Venus, mRFP1	[139]
RIPK1 and RIPK3	Necroptosis	–	[140]
Atg4A and Atg4B	Autophagy	CFP, YFP	[141]
MT-MMP1	ECM – remodeling	Ypet, ECFP	[142]
MT-MMP1	ECM – remodeling	Orange2, Cherry	[143]

determine the activation of specific proteases, often following the stimulation of a pathway. For example, in the case of the caspase-3 biosensor, in the presence of active enzyme, the single-peptide sensor DEVD (caspase cleavage sequence) is cleaved, increasing the distance between CFP and eYFP, resulting in increased CFP fluorescence and decreased FRET [136]. Another major limitation is that measuring loss of signal is a readout for measuring FRET rather than measuring an increase in signal, which is preferred for most biological studies (Table 5).

3.3.3 Conformational Change-Based FRET Biosensors

FRET biosensors for measuring conformational changes in proteins and other macromolecules are the most prevalent subclass, followed by cleavage-based FRET biosensors. The ability of a protein to form a structural conformation that can execute its biological function is the driving factor for these FRET biosensors. Such conformational changes are also contributed to a large extent by posttranslational modifications such as phosphorylation, glycosylation, ubiquitination, S-nitrosylation, methylation, acetylation, lipidation, sumoylation, and proteolysis. An advantage of a conformational change specific sensor is that upon design optimization and validation for a specific analyte, it lends flexibility to cover a wide range of biological processes. The conformational change-based biosensors are also reversible, which offers new avenues for dynamic analyte sensing. For example, regarding the glucose biosensor, the glucose-/galactose-binding protein MglB (D-galactose-binding periplasmic protein, from *E. coli*), consisting of two lobes and a hinge region, is coupled terminally with a CFP and a YFP. The binding of glucose to the sensor leads to increase in FRET signal [144] (Table 6).

3.3.4 Mechanical Force-Based FRET Biosensors

The three-dimensional structure of a protein can be changed not only by modifying the protein itself but also by applying an external mechanical force. A good example for this would be the proteins contained in spider silk. These often feature helical

Table 6 Conformational change-based FRET biosensors

Target	Type	FRET pair	Reference
CyclinB1-Cdk1	Cell division	mCerulean, Ypet	[145]
AKT	Signal transduction	ECFP, Ypet	[146]
AKT-PDK1	Mechano-transduction	CFP, YFP	[147]
FAK	Mechano-transduction	ECFP, Ypet	[148]
Src	Mechano-transduction	ECFP, EYFP	[149]
ATP	Metabolite quantification	GFP, OFP	[150]
Glucose	Metabolite quantification	EYFP, ECFP	[151]
Lactate	Metabolite quantification	mTFP, Venus	[152]
Ca^{2+}	Metabolite quantification	BFP, GFP	[153]
BCR-ABL	Drug efficacy	M1Venus, ECFP	[154]
Src	Drug efficacy	ECFP, EYFP	[155]
ZAP-70	T-cell interaction	CFP, YFP	[156]
Lck	T-cell interaction	ECFP, EYFP	[157]

Table 7 Mechanical force-based FRET biosensors

Target	Type	FRET pair	Reference
Vinculin	Focal adhesion	mTFP1, Venus	[158]
VE-cadherin, PECAM-1	Fluid shear stress	mTFP1, Venus	[159]
E-cadherin	Fluid shear stress	mTFP1, Venus	[160]

segments which can stretch out to a great extent, giving the thread its elasticity. Mechanical forces (such as tension) not only are a stress to cells but play a central role in many developmental, physiological, and pathological processes, especially regarding the transduction of signals. One of the exciting results in this field was produced by Grashoff et al., who have designed a tension sensor module (TSMod) to examine the mechanical forces across vinculin during cell migration [158]. In this sensor, a 40-amino-acid-long elastic domain was inserted between two fluorophores (mTFP1 and Venus (A206K)) as a potential fluorescence resonance energy transfer (FRET) pair. The elastic domain derived from the spider silk protein flagelliform consists of repetitive amino acid motifs that form entropic nanosprings suitable for measuring piconewton forces. Since FRET is highly sensitive to the distance between the fluorophores, FRET efficiency changes under tension (Table 7).

3.3.5 FRET Sensors for Assessing Microenvironmental Changes

The three classes of biosensors discussed in the preceding section manifest decrease or increase in FRET upon change in distance between donor and acceptor, whereas microenvironment-responsive FRET sensors exploit the sensitivity of a fluorophore to certain microenvironmental conditions. One such microenvironment-sensitive fluorescent protein is YFP, which makes it a promising choice as one of the FRET pairs. For example, the oxygen biosensor FluBO for detecting intracellular oxygen

Table 8 Microenvironment-based FRET biosensors

Type	Target	FRET pair	Reference
Oxygen and reactive oxygen species (ROS)	Oxygen	YFP, FbFP	[161]
Oxygen and ROS	ROS	ECFP, EYFP	[163]
pH	pH	GFP, YFP	[164]
pH	pH	ECFP, EYFP	[165]

uses an oxygen-insensitive donor fluorescent protein FbFP (hypoxia-tolerant flavin-binding fluorescent protein) that is intramolecularly linked to an oxygen-sensitive acceptor fluorescent protein, and thus FRET only occurs in the presence of oxygen [161]. Blood flow, oxygen delivery and consumption, and hypoxia are important aspects of in vivo cancer biology. The dual imaging of these factors that may influence tumor behavior with altered drug target signaling could potentially be co-monitored using these distinct but interdependent types of FRET biosensor readouts [162] (Table 8).

3.4 Translocation Sensors/Assays

A unique field of application for FP sensors is in tracking the redistribution of proteins between different cellular compartments such as the nucleus, endosome, membrane, cytosol, and mitochondria [166, 167]. The translocation of proteins between cellular compartments in response to different external stimuli has been considered common phenomenon that involves protein redistribution into different compartments of the living cells. Tracking proteins and their distribution patterns opens up the possibility of monitoring the activity of various signaling pathways and associated intracellular events. Fusion of proteins such as phosphatases, transcription factors, receptors, and kinases with fluorescent proteins can act as ready-to-use translocation sensors for deduction of cellular metabolic and biogenesis pathways. Such a fusion construct can localize outside or inside the nucleus, or on the cell membrane, cytosol, endosome, etc., and such protein trafficking can be monitored in real time with the help of translocation sensors. These sensors are reversible, enabling time-dependent tracking of specific proteins in various cellular compartments. In this context, the spatial and functional division into the two dynamic intracellular compartments, i.e., nucleus and the cytoplasm, can easily be distinguished using microscopy. Modern microscopy platforms enable high-content screening using translocating FPs.

In such high-throughput screening assays, screened compounds can be assessed for their potential effects on protein translocation or used to study the inhibition of

protein translocation in response to an agonist or external stimuli. A combination of high-resolution microscopy and advanced image recognition software enables quantitative analysis of translocation events with reliable information on the efficiency of the influencing stimulus. Recently Fetz et al. have developed three classes of modular protein translocation biosensors tailored to investigate (1) signal-mediated nucleocytoplasmic transport, (2) protease activity, and (3) protein-protein interactions [168]. Besides the mapping of protein function, the biosensors can also be applied to identify chemicals and/or (nano)materials modulating the respective protein activities and be used for RNAi-mediated genetic screens. In general, the rapidly developing field of translocation sensors appears very promising both for basic science studies and in drug development applications.

4 Advances in Biosensors for Animal Imaging

Whole-body animal imaging with fluorescent proteins has been shown to be a powerful technology to develop various disease models. The red-shifted proteins with brighter emission wavelengths are preferred candidates for in vivo models as they are more sensitive owing to the reduced light absorption by tissue with much lower scattering. For example, a protein called Katushka driven by the hybrid CAG promoter activated upon Cre-mediated recombination has been developed by Hurtado et al., for deep tissue imaging in mice models. This group successfully demonstrated the expression of Katushka exclusively in a specific cell population within the deep animal body such as pancreatic beta cells which can be monitored by noninvasive whole-body imaging [169]. The implication of imaging biosensors in animal studies is severely affected by the level of biosensors expression and the wavelength of fluorescent proteins used for imaging [170]. For example, Audet et al. [171] have developed a double transgenic mouse line co-expressing the beta-2 adrenergic receptor fused to *Renilla luciferase* (beta(2)AR-Rluc) and beta-arrestin-2 fused to a green fluorescent protein (GFP2-beta arr2). Although the two halves of a bimolecular reporter are driven by the same ostensibly ubiquitous reporter, the first reporter was expressed reasonably brighter in a number of tissue types, whereas the second reporter appeared only in testes. In addition, the low-level expression of sensors with tissue-specific promoters further hampers the in vivo imaging ability of sensors constructed using fluorescent proteins. The effective FRET studies also cannot be carried out in vivo because of extremely low SNRs. The implication of a fluorescent protein for whole-body imaging is largely determined by the emission region and the brightness. Transgenic animal models with fluorescent proteins have been utilized for tracking tumor growth and metastasis, gene expression, angiogenesis, and bacterial infection even at subcellular resolution depending on the position of the cells in the animal [172]. Deep tissue imaging in animal models has been severely limited by the interference by skin autofluorescence. Apart from this, in few instances, overexpression of biosensors also leads to unintended changes like embryonic lethality or even perturbation of the physiological relevance of the sensor

[173]. However, with recent progress in CRISPR/Cas9 genome engineering techniques, it has become possible to edit more precisely the genomes of diverse cell types and organisms and routinely insert fluorescent protein tags into endogenous genomic loci in some organisms. Hara et al. [173] reported expression of an endoplasmic reticulum (ER) Ca^{2+} biosensor in transgenic mouse pancreas. The expression of a yellow cameleon3.3er (YC3.3er) transgene with mouse insulin 1 promoter was limited to pancreatic beta cells within islets of Langerhans and absent in the exocrine pancreas and other tissues [173]. The study established that by controlling transgene transcription with a cell-specific promoter, transgenic expression of FRET-based Ca^{2+} sensors can be incorporated in mammals to facilitate real-time optical imaging of signal transduction events in living tissues. Yang et al. developed a red fluorescent protein-based cAMP indicator named "Pink Flamindo" which could effectively trace the spatiotemporal dynamics of intracellular cAMP generated by photoactivated adenylate cyclase in response to light and in dual-color imaging studies using a green Ca^{2+} indicator.

The elevation of cAMP levels in vivo in cerebral cortical astrocytes was successfully monitored by two-photon imaging. The cAMP-PKA signaling pathway plays a key role in the excitability of neurons. In order to study its role, protein kinase A (PKA) expression in neurons has been mapped in whole-brain context in live animals. In a study by Gervasi et al., in vivo multiphoton imaging was used to measure the dynamics of PKA responses to dopamine and octopamine in the MB neurons of living flies. The PKA activity was monitored on real-time basis by using the genetically encoded FRET probe AKAR2 [133]. The AKAR2 probe is based on yeast-derived phosphothreonine-binding domain (FHA1) and an optimized PKA substrate domain. The substrate domain upon phosphorylation by PKA interacts with the binding pocket of the FHA1 domain, increasing the FRET between two GFP variants CFP and citrine [174]. A recent study by Sun et al. developed a genetically encoded GPCR-activation-based-DA (GRAB DA) sensors to measure DA changes reliably and specifically with high spatiotemporal precision in *Drosophila* (Fig. 5ii) [175]. The GRAB DA sensor could resolve a single-electrical-stimulus-evoked DA release in mouse brain slices and detect endogenous DA release in living flies with subcellular resolution, sub-second kinetics, and excellent molecular specificity. Similarly, Portugues et al. studied the dynamics and spatial distribution of neuronal activities during optokinetic response in zebra fish larvae. The whole-brain activity dynamics was assigned by specific hue based on the timing of its response relative to the stimulus, which enabled categorization of brain regions into distinct response-based functional modules (Fig. 5iii) [176]. Another recent technique is called "Brainbow" that used the combinatorial expression of a series of four different color fluorescent proteins resulting in at least 90 different colors of cells in the brain such that the lineage of each neuron can be traced [177]. For translational purposes, mammalian systems such as mouse are appealing targets for similar in vivo studies. However, there are a number of challenges for in vivo kinase studies, particularly in living mice. A RhoA-FRET biosensor-based transgenic mouse was recently developed by Nobis et al., for real-time longitudinal, intravital imaging of RhoA deregulation in invasive mammary and pancreatic cancers [178].

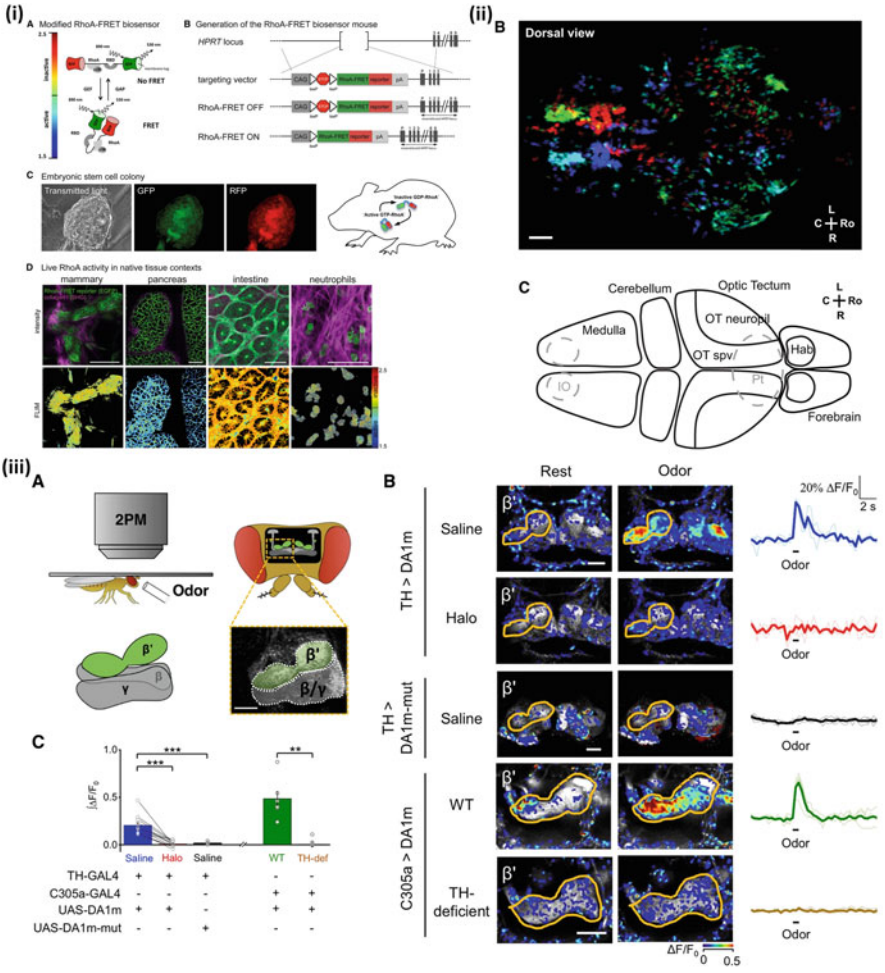

Fig. 5 (*i*) Generation of the RhoA-FRET biosensor mouse: (**a**) schematic of the Raichu-RhoA biosensor; (**b**) targeted to the Hprt locus to generate the RhoA-FRET biosensor mouse. (**c**) Embryonic stem cell colony expressing the RhoA-FRET biosensor (GFP, green; RFP, red). (**d**) RhoA activity in the mammary fat pad, pancreas, intestine, and neutrophils of RhoA-ON mice. (*ii*) In vivo imaging of DA dynamics in the *Drosophila* brain: (**a**) schematic for odor stimulation during two-photon microscopy in *Drosophila*. (**b**) Fluorescence changes of DA1m- or DA1m-mut-expressing flies to 1 s of odor stimulation. (**c**) Group analysis of the odor-evoked fluorescence responses. (*iii*) Clustering of fluorescence traces reveals four temporal clusters in zebra fish; anatomical distribution of activity clusters in one fish. Sum projection showing the distribution of the four clusters of activity in the same fish (top), with colors corresponding to the color traces (bottom). Scale bar 50 μm. (Figures in different panels are reproduced with permission from (*i*) Cell Rep. 2017 Oct 3;21(1):274–288 [178]; (*ii*) Cell. 2018 Jul 12;174(2):481–496 [175]; (*iii*) Neuron. 2014 Mar 19;81(6):1328–1343 [176])

Apart from mice, *Caenorhabditis elegans* is a widely used animal model for studying neurodegenerative disorders. Transgenic *C. elegans* strains expressing green, yellow, or red fluorescent proteins in embryos were developed by Heppert et al., to image embryos expressing fluorescent proteins under the same conditions with probe mNeonGreen. Monomeric green (GFP, mNeonGreen [mNG]), yellow (mNG, monomeric yellow fluorescent protein for energy transfer [mYPet]), and red (TagRFP-T, mRuby2, mCherry, mKate2) fluorescent proteins were evaluated for comparative in vivo experiments in *C. elegans* [179]. Since *C. elegans* is a transparent small animal, fluorescent protein-based sensors provide sensitive imaging ability to track its biological events in a much better way compared to large animals. Hirayama et al. designed a first-generation near-IR turn-on fluorescent sensor, CS790AM, to report dynamic copper fluctuations in vivo and detected the basal, endogenous levels of exchangeable copper in living mice platform to monitor labile copper pools role in murine Wilson's disease model [180].

5 Drawbacks Associated with the Use of Fluorescent Proteins in Biosensors

Although fluorescent protein-based biosensors offer a realistic, cost-effective, and high-throughput imaging approach for studying various biological processes of cells, their application is also limited by the inherent problem of photobleaching, phototoxicity, low quantum yield, high background signal, and especially tissue attenuation in in vivo imaging applications. Upon repeated cycles of excitation, the fluorophore of the sensor protein gets damaged and leads to loss of fluorescence signal which can result in non-specific sensor signal. In addition, it severely limits the application of fluorescent protein biosensors for real-time imaging where time-dependent pattern of biosensor signal is important for achieving reliable result for the studies [181, 182]. On the other hand, exposure to higher-energy photons tends to generate reactive oxygen species (ROS) which are highly reactive species capable of inflicting damage to cellular biomolecules like DNA, RNA, and proteins by oxidation, which in turn limits the possibilities of multiplexing the assays in in vitro and in vivo imaging applications [183]. In the event of avoiding photobleaching and phototoxicity, the narrow operation bandwidth and shorter imaging time leave us with lower quantum yield of these fluorescent proteins with limited sensitivity. The cells by itself possess biomolecules that prominently contribute to autofluorescence and render high background while imaging such fluorescent proteins with low quantum yield, which limits the spectral resolution and sensitivity of the biosensor [184, 185]. To overcome the limitation of tissue attenuation, the development of fluorescent proteins with high quantum yields and far-red or near-infrared (NIR) shifted absorption and emission wavelengths are preferred. Currently there are several fluorescent protein variants which emit light in the NIR range and have been developed from bacterial phytochrome photoreceptors and are used in various biosensor applications [186, 187].

6 Conclusion and Future Perspectives

The course of evolution of fluorescent proteins from the first known member GFP to a completely new family of fluorescent proteins spanning across the visible spectra has emerged in relatively short time span. The rapid growth and applications of the FP repertoire for in vivo imaging continuously shed light on studying crucial cellular events which play a vital role in development and progression of diseases. With the present capabilities of FPs, multicolor labeling of proteins and nucleic acids; tracking of protein movements, interactions, activities, degradation, organelle motility, and fusion-fission events; and monitoring of promoter activation, as well as multiparameter imaging of various cellular processes, including changes in concentration of signal molecules, changes of membrane potential and cell state, etc., can be deduced efficiently. Although extensive variants of biosensors for specific applications have been developed, it is expected that further improvements in brightness, photostability, maturation rate, pH stability, and performance in fusions will gain priority in the future. Even though a significant progress has been made in the demonstration of novel fluorescent protein-based biosensors for in vivo models, further research is required to establish consistent, reproducible, and reliable imaging instruments with far-red shifted fluorescent proteins, and animal models for disease investigations. Although rapid strides have been made in this field, further improvements on deep tissue imaging with higher sensitivity and long-term noninvasive imaging would open wide range of applications for biosensors. Addressing the drawback of loss of fluorescent proteins during tissue fixation or subsequent processing can also improve ex vivo histopathological analysis of tissues from transgenic animals.

Acknowledgments We would like to thank the Canary Center at Stanford, Department of Radiology, for providing facility and resources. We also thank SCi3 Small Animal Imaging Service Center, Stanford University School of Medicine, for providing imaging facilities and data analysis support. We acknowledge Dr. Sanjiv Sam Gambhir, Chair of the Department of Radiology, Stanford University, for his constant support and help.

Compliance with Ethical Standards

Conflicts of Interest There are no actual or potential conflicts of interest in regard to this chapter.

Funding This research was supported by NIH R01CA209888 and NIH R21EB022298. This work was also in part supported by the Center for Cancer Nanotechnology Excellence for Translational Diagnostics (CCNE-TD) at Stanford University through an award (grant no. U54 CA199075) from the National Cancer Institute (NCI) of the National Institutes of Health (NIH).

Ethical Approval All applicable international, national, and/or institutional guidelines for the care and use of animals were followed.

References

1. Bu L, Shen B, Cheng Z (2014) Fluorescent imaging of cancerous tissues for targeted surgery. Adv Drug Deliv Rev 76:21–38
2. Lavis LD, Raines RT (2008) Bright ideas for chemical biology. ACS Chem Biol 3(3):142–155
3. Tsien RY (2010) Nobel lecture: constructing and exploiting the fluorescent protein paintbox. Integr Biol 2(2–3):77–93
4. Vigneshvar S et al (2016) Recent advances in biosensor technology for potential applications – an overview. Front Bioeng Biotechnol 4:11
5. Shimomura O, Johnson FH, Saiga Y (1962) Extraction, purification and properties of aequorin, a bioluminescent protein from the luminous hydromedusan, Aequorea. J Cell Comp Physiol 59:223–239
6. Gong Z, Ju B, Wan H (2001) Green fluorescent protein (GFP) transgenic fish and their applications. Genetica 111(1–3):213–225
7. Lai L et al (2002) Transgenic pig expressing the enhanced green fluorescent protein produced by nuclear transfer using colchicine-treated fibroblasts as donor cells. Mol Reprod Dev 62 (3):300–306
8. Dhandayuthapani S et al (1995) Green fluorescent protein as a marker for gene expression and cell biology of mycobacterial interactions with macrophages. Mol Microbiol 17(5):901–912
9. Zacharias DA et al (2002) Partitioning of lipid-modified monomeric GFPs into membrane microdomains of live cells. Science 296(5569):913–916
10. McCombs JE, Palmer AE (2008) Measuring calcium dynamics in living cells with genetically encodable calcium indicators. Methods 46(3):152–159
11. Mank M, Griesbeck O (2008) Genetically encoded calcium indicators. Chem Rev 108 (5):1550–1564
12. Xiao T et al (2017) In vivo analysis with electrochemical sensors and biosensors. Anal Chem 89(1):300–313
13. Takanaga H, Chaudhuri B, Frommer WB (2008) GLUT1 and GLUT9 as major contributors to glucose influx in HepG2 cells identified by a high sensitivity intramolecular FRET glucose sensor. Biochim Biophys Acta 1778(4):1091–1099
14. Ha JS et al (2007) Design and application of highly responsive fluorescence resonance energy transfer biosensors for detection of sugar in living Saccharomyces cerevisiae cells. Appl Environ Microbiol 73(22):7408–7414
15. Hires SA, Zhu Y, Tsien RY (2008) Optical measurement of synaptic glutamate spillover and reuptake by linker optimized glutamate-sensitive fluorescent reporters. Proc Natl Acad Sci U S A 105(11):4411–4416
16. Tainaka K et al (2010) Design strategies of fluorescent biosensors based on biological macromolecular receptors. Sensors 10(2):1355–1376
17. Mehrotra P (2016) Biosensors and their applications – a review. J Oral Biol Craniofac Res 6(2):153–159
18. Bajar BT et al (2016) A guide to fluorescent protein FRET pairs. Sensors 16(9):1488
19. Laverdant J et al (2011) Experimental determination of the fluorescence quantum yield of semiconductor nanocrystals. Materials 4(7):1182–1193
20. Rurack K, Spieles M (2011) Fluorescence quantum yields of a series of red and near-infrared dyes emitting at 600-1000 nm. Anal Chem 83(4):1232–1242
21. Verma D, Grigoryan G, Bailey-Kellogg C (2015) Structure-based design of combinatorial mutagenesis libraries. Protein Sci 24(5):895–908
22. Saito Y et al (2018) Machine-learning-guided mutagenesis for directed evolution of fluorescent proteins. ACS Synth Biol 7(9):2014–2022
23. Mitchell JA et al (2016) Rangefinder: a semisynthetic FRET sensor design algorithm. ACS Sensors 1(11):1286–1290
24. Malakauskas SM, Mayo SL (1998) Design, structure and stability of a hyperthermophilic protein variant. Nat Struct Biol 5(6):470–475

25. Looger LL et al (2003) Computational design of receptor and sensor proteins with novel functions. Nature 423(6936):185–190
26. Jiang L et al (2008) De novo computational design of retro-aldol enzymes. Science 319(5868):1387–1391
27. Rothlisberger D et al (2008) Kemp elimination catalysts by computational enzyme design. Nature 453(7192):190–195
28. Kuhlman B et al (2003) Design of a novel globular protein fold with atomic-level accuracy. Science 302(5649):1364–1368
29. Yang F, Moss LG, Phillips Jr GN (1996) The molecular structure of green fluorescent protein. Nat Biotechnol 14(10):1246–1251
30. Heim R, Prasher DC, Tsien RY (1994) Wavelength mutations and posttranslational autoxidation of green fluorescent protein. Proc Natl Acad Sci U S A 91(26):12501–12504
31. Heim R, Tsien RY (1996) Engineering green fluorescent protein for improved brightness, longer wavelengths and fluorescence resonance energy transfer. Curr Biol 6(2):178–182
32. Tomosugi W et al (2009) An ultramarine fluorescent protein with increased photostability and pH insensitivity. Nat Methods 6(5):351–353
33. Kremers GJ et al (2006) Cyan and yellow super fluorescent proteins with improved brightness, protein folding, and FRET Forster radius. Biochemistry 45(21):6570–6580
34. Rizzo MA et al (2004) An improved cyan fluorescent protein variant useful for FRET. Nat Biotechnol 22(4):445–449
35. Cormack BP, Valdivia RH, Falkow S (1996) FACS-optimized mutants of the green fluorescent protein (GFP). Gene 173(1):33–38
36. Heim R, Cubitt AB, Tsien RY (1995) Improved green fluorescence. Nature 373 (6516):663–664
37. Yang TT, Cheng L, Kain SR (1996) Optimized codon usage and chromophore mutations provide enhanced sensitivity with the green fluorescent protein. Nucleic Acids Res 24 (22):4592–4593
38. Ormo M et al (1996) Crystal structure of the Aequorea victoria green fluorescent protein. Science 273(5280):1392–1395
39. Gittins JR et al (2015) Fluorescent protein-mediated colour polymorphism in reef corals: multicopy genes extend the adaptation/acclimatization potential to variable light environments. Mol Ecol 24(2):453–465
40. Lukyanov KA et al (2000) Natural animal coloration can be determined by a nonfluorescent green fluorescent protein homolog. J Biol Chem 275(34):25879–25882
41. Matz MV et al (1999) Fluorescent proteins from nonbioluminescent Anthozoa species. Nat Biotechnol 17(10):969–973
42. Shkrob MA et al (2005) Far-red fluorescent proteins evolved from a blue chromoprotein from Actinia equina. Biochem J 392(Pt 3):649–654
43. Evdokimov AG et al (2006) Structural basis for the fast maturation of Arthropoda green fluorescent protein. EMBO Rep 7(10):1006–1012
44. Shagin DA et al (2004) GFP-like proteins as ubiquitous metazoan superfamily: evolution of functional features and structural complexity. Mol Biol Evol 21(5):841–850
45. Germond A et al (2016) Design and development of genetically encoded fluorescent sensors to monitor intracellular chemical and physical parameters. Biophys Rev 8(2):121–138
46. Tavare JM, Fletcher LM, Welsh GI (2001) Using green fluorescent protein to study intracellular signalling. J Endocrinol 170(2):297–306
47. Palmer AE et al (2011) Design and application of genetically encoded biosensors. Trends Biotechnol 29(3):144–152
48. Day RN, Davidson MW (2009) The fluorescent protein palette: tools for cellular imaging. Chem Soc Rev 38(10):2887–2921
49. Song W, Strack RL, Jaffrey SR (2013) Imaging bacterial protein expression using genetically encoded RNA sensors. Nat Methods 10(9):873–875
50. Thorn K (2017) Genetically encoded fluorescent tags. Mol Biol Cell 28(7):848–857

51. Rowland CE et al (2015) Intracellular FRET-based probes: a review. Methods Appl Fluoresc 3 (4):042006
52. Miesenbock G, De Angelis DA, Rothman JE (1998) Visualizing secretion and synaptic transmission with pH-sensitive green fluorescent proteins. Nature 394(6689):192–195
53. Johnson DE et al (2009) Red fluorescent protein pH biosensor to detect concentrative nucleoside transport. J Biol Chem 284(31):20499–20511
54. Tallini YN et al (2006) Imaging cellular signals in the heart in vivo: cardiac expression of the high-signal Ca2+ indicator GCaMP2. Proc Natl Acad Sci U S A 103(12):4753–4758
55. Souslova EA et al (2007) Single fluorescent protein-based Ca2+ sensors with increased dynamic range. BMC Biotechnol 7:37
56. Griesbeck O et al (2001) Reducing the environmental sensitivity of yellow fluorescent protein. Mechanism and applications. J Biol Chem 276(31):29188–29194
57. Belousov VV et al (2006) Genetically encoded fluorescent indicator for intracellular hydrogen peroxide. Nat Methods 3(4):281–286
58. Gallegos LL, Kunkel MT, Newton AC (2006) Targeting protein kinase C activity reporter to discrete intracellular regions reveals spatiotemporal differences in agonist-dependent signaling. J Biol Chem 281(41):30947–30956
59. Goedhart J et al (2007) Sensitive detection of p65 homodimers using red-shifted and fluorescent protein-based FRET couples. PLoS One 2(10):e1011
60. Miyawaki A et al (1997) Fluorescent indicators for Ca2+ based on green fluorescent proteins and calmodulin. Nature 388(6645):882–887
61. Berney C, Danuser G (2003) FRET or no FRET: a quantitative comparison. Biophys J 84 (6):3992–4010
62. Hanson GT et al (2002) Green fluorescent protein variants as ratiometric dual emission pH sensors. 1. Structural characterization and preliminary application. Biochemistry 41 (52):15477–15488
63. Kneen M et al (1998) Green fluorescent protein as a noninvasive intracellular pH indicator. Biophys J 74(3):1591–1599
64. Jayaraman S et al (2000) Mechanism and cellular applications of a green fluorescent protein-based halide sensor. J Biol Chem 275(9):6047–6050
65. DiPilato LM, Cheng X, Zhang J (2004) Fluorescent indicators of cAMP and Epac activation reveal differential dynamics of cAMP signaling within discrete subcellular compartments. Proc Natl Acad Sci U S A 101(47):16513–16518
66. Hanson GT et al (2004) Investigating mitochondrial redox potential with redox-sensitive green fluorescent protein indicators. J Biol Chem 279(13):13044–13053
67. Ashby MC, Ibaraki K, Henley JM (2004) It's green outside: tracking cell surface proteins with pH-sensitive GFP. Trends Neurosci 27(5):257–261
68. Llopis J et al (1998) Measurement of cytosolic, mitochondrial, and Golgi pH in single living cells with green fluorescent proteins. Proc Natl Acad Sci U S A 95(12):6803–6808
69. Sankaranarayanan S et al (2000) The use of pHluorins for optical measurements of presynaptic activity. Biophys J 79(4):2199–2208
70. Henderson JN et al (2009) Excited state proton transfer in the red fluorescent protein mKeima. J Am Chem Soc 131(37):13212–13213
71. Violot S et al (2009) Reverse pH-dependence of chromophore protonation explains the large Stokes shift of the red fluorescent protein mKeima. J Am Chem Soc 131(30):10356–10357
72. Fang EF et al (2017) In vitro and in vivo detection of mitophagy in human cells, C. Elegans, and mice. J Vis Exp 129:e56301
73. Shinoda H, Shannon M, Nagai T (2018) Fluorescent proteins for investigating biological events in acidic environments. Int J Mol Sci 19(6):1543
74. Tantama M, Hung YP, Yellen G (2011) Imaging intracellular pH in live cells with a genetically encoded red fluorescent protein sensor. J Am Chem Soc 133(26):10034–10037
75. Shcherbakova DM, Subach OM, Verkhusha VV (2012) Red fluorescent proteins: advanced imaging applications and future design. Angew Chem Int Ed Engl 51(43):10724–10738

76. Horikawa K et al (2010) Spontaneous network activity visualized by ultrasensitive Ca(2+) indicators, yellow Cameleon-Nano. Nat Methods 7(9):729–732
77. Nagai T et al (2004) Expanded dynamic range of fluorescent indicators for Ca(2+) by circularly permuted yellow fluorescent proteins. Proc Natl Acad Sci U S A 101 (29):10554–10559
78. Palmer AE et al (2004) Bcl-2-mediated alterations in endoplasmic reticulum Ca2+ analyzed with an improved genetically encoded fluorescent sensor. Proc Natl Acad Sci U S A 101 (50):17404–17409
79. Palmer AE et al (2006) Ca2+ indicators based on computationally redesigned calmodulin-peptide pairs. Chem Biol 13(5):521–530
80. Mank M et al (2008) A genetically encoded calcium indicator for chronic in vivo two-photon imaging. Nat Methods 5(9):805–811
81. Vinkenborg JL et al (2009) Genetically encoded FRET sensors to monitor intracellular Zn2+ homeostasis. Nat Methods 6(10):737–740
82. Evers TH et al (2007) Ratiometric detection of Zn(II) using chelating fluorescent protein chimeras. J Mol Biol 374(2):411–425
83. Qin Y et al (2011) Measuring steady-state and dynamic endoplasmic reticulum and Golgi Zn2+ with genetically encoded sensors. Proc Natl Acad Sci U S A 108(18):7351–7356
84. Emmanouilidou E et al (1999) Imaging Ca2+ concentration changes at the secretory vesicle surface with a recombinant targeted cameleon. Curr Biol 9(16):915–918
85. Palmer AE, Tsien RY (2006) Measuring calcium signaling using genetically targetable fluorescent indicators. Nat Protoc 1(3):1057–1065
86. Kerppola TK (2008) Bimolecular fluorescence complementation (BiFC) analysis as a probe of protein interactions in living cells. Annu Rev Biophys 37:465–487
87. Kerppola TK (2008) Bimolecular fluorescence complementation: visualization of molecular interactions in living cells. Methods Cell Biol 85:431–470
88. Kodama Y, Hu CD (2012) Bimolecular fluorescence complementation (BiFC): a 5-year update and future perspectives. Biotechniques 53(5):285–298
89. Kerppola TK (2006) Visualization of molecular interactions by fluorescence complementation. Nat Rev Mol Cell Biol 7(6):449–456
90. Magliery TJ et al (2005) Detecting protein-protein interactions with a green fluorescent protein fragment reassembly trap: scope and mechanism. J Am Chem Soc 127(1):146–157
91. Hu CD, Chinenov Y, Kerppola TK (2002) Visualization of interactions among bZIP and Rel family proteins in living cells using bimolecular fluorescence complementation. Mol Cell 9 (4):789–798
92. Hu CD, Kerppola TK (2003) Simultaneous visualization of multiple protein interactions in living cells using multicolor fluorescence complementation analysis. Nat Biotechnol 21 (5):539–545
93. Shyu YJ et al (2006) Identification of new fluorescent protein fragments for bimolecular fluorescence complementation analysis under physiological conditions. Biotechniques 40 (1):61–66
94. Waadt R et al (2008) Multicolor bimolecular fluorescence complementation reveals simultaneous formation of alternative CBL/CIPK complexes in planta. Plant J 56(3):505–516
95. Fan JY et al (2008) Split mCherry as a new red bimolecular fluorescence complementation system for visualizing protein-protein interactions in living cells. Biochem Biophys Res Commun 367(1):47–53
96. Kodama Y, Wada M (2009) Simultaneous visualization of two protein complexes in a single plant cell using multicolor fluorescence complementation analysis. Plant Mol Biol 70 (1–2):211–217
97. Chu J et al (2009) A novel far-red bimolecular fluorescence complementation system that allows for efficient visualization of protein interactions under physiological conditions. Biosens Bioelectron 25(1):234–239

98. Grinberg AV, Hu CD, Kerppola TK (2004) Visualization of Myc/Max/Mad family dimers and the competition for dimerization in living cells. Mol Cell Biol 24(10):4294–4308
99. Vidi PA et al (2008) Ligand-dependent oligomerization of dopamine D(2) and adenosine A (2A) receptors in living neuronal cells. Mol Pharmacol 74(3):544–551
100. Niu W, Guo J (2013) Expanding the chemistry of fluorescent protein biosensors through genetic incorporation of unnatural amino acids. Mol Biosyst 9(12):2961–2970
101. Ayyadurai N et al (2011) Development of a selective, sensitive, and reversible biosensor by the genetic incorporation of a metal-binding site into green fluorescent protein. Angew Chem Int Ed Engl 50(29):6534–6537
102. Niu W, Guo J (2017) Novel fluorescence-based biosensors incorporating unnatural amino acids. Methods Enzymol 589:191–219
103. Wang F et al (2012) Unnatural amino acid mutagenesis of fluorescent proteins. Angew Chem Int Ed Engl 51(40):10132–10135
104. Chen S et al (2012) Reaction-based genetically encoded fluorescent hydrogen sulfide sensors. J Am Chem Soc 134(23):9589–9592
105. Chen ZJ et al (2013) Genetically encoded fluorescent probe for the selective detection of peroxynitrite. J Am Chem Soc 135(40):14940–14943
106. Alford SC et al (2012) A fluorogenic red fluorescent protein heterodimer. Chem Biol 19 (3):353–360
107. Alford SC et al (2012) Dimerization-dependent green and yellow fluorescent proteins. ACS Synth Biol 1(12):569–575
108. Thornton JM, Sibanda BL (1983) Amino and carboxy-terminal regions in globular proteins. J Mol Biol 167(2):443–460
109. Bliven S, Prlic A (2012) Circular permutation in proteins. PLoS Comput Biol 8(3):e1002445
110. Miyawaki A et al (1999) Dynamic and quantitative Ca2+ measurements using improved cameleons. Proc Natl Acad Sci U S A 96(5):2135–2140
111. Tian L, Hires SA, Looger LL (2012) Imaging neuronal activity with genetically encoded calcium indicators. Cold Spring Harb Protoc 2012(6):647–656
112. Nakai J, Ohkura M, Imoto K (2001) A high signal-to-noise Ca(2+) probe composed of a single green fluorescent protein. Nat Biotechnol 19(2):137–141
113. Nausch LW et al (2008) Differential patterning of cGMP in vascular smooth muscle cells revealed by single GFP-linked biosensors. Proc Natl Acad Sci U S A 105(1):365–370
114. Mizuno T et al (2007) Metal-ion-dependent GFP emission in vivo by combining a circularly permutated green fluorescent protein with an engineered metal-ion-binding coiled-coil. J Am Chem Soc 129(37):11378–11383
115. Mao T et al (2008) Characterization and subcellular targeting of GCaMP-type genetically-encoded calcium indicators. PLoS One 3(3):e1796
116. Suzuki J, Kanemaru K, Iino M (2016) Genetically encoded fluorescent indicators for organellar calcium imaging. Biophys J 111(6):1119–1131
117. Baird GS, Zacharias DA, Tsien RY (1999) Circular permutation and receptor insertion within green fluorescent proteins. Proc Natl Acad Sci U S A 96(20):11241–11246
118. Nagai T et al (2001) Circularly permuted green fluorescent proteins engineered to sense Ca2+. Proc Natl Acad Sci U S A 98(6):3197–3202
119. Ohkura M et al (2005) Genetically encoded bright Ca2+ probe applicable for dynamic Ca2+ imaging of dendritic spines. Anal Chem 77(18):5861–5869
120. Kawai Y, Sato M, Umezawa Y (2004) Single color fluorescent indicators of protein phosphorylation for multicolor imaging of intracellular signal flow dynamics. Anal Chem 76 (20):6144–6149
121. Gautam SG et al (2009) Exploration of fluorescent protein voltage probes based on circularly permuted fluorescent proteins. Front Neuroeng 2:14
122. Knopfel T et al (2003) Optical recordings of membrane potential using genetically targeted voltage-sensitive fluorescent proteins. Methods 30(1):42–48

123. Berg J, Hung YP, Yellen G (2009) A genetically encoded fluorescent reporter of ATP:ADP ratio. Nat Methods 6(2):161–166
124. Hernandez-Barrera A et al (2015) Hyper, a hydrogen peroxide sensor, indicates the sensitivity of the Arabidopsis root elongation zone to aluminum treatment. Sensors 15(1):855–867
125. Niethammer P et al (2009) A tissue-scale gradient of hydrogen peroxide mediates rapid wound detection in zebrafish. Nature 459(7249):996–999
126. Forster T (1946) Energiewanderung und Fluoreszenz. Naturwissenschaften 33(6):166–175
127. Ma L, Yang F, Zheng J (2014) Application of fluorescence resonance energy transfer in protein studies. J Mol Struct 1077:87–100
128. Tamura T, Hamachi I (2014) Recent progress in design of protein-based fluorescent biosensors and their cellular applications. ACS Chem Biol 9(12):2708–2717
129. Day RN, Davidson MW (2012) Fluorescent proteins for FRET microscopy: monitoring protein interactions in living cells. Bioessays 34(5):341–350
130. Nikolaev VO, Gambaryan S, Lohse MJ (2006) Fluorescent sensors for rapid monitoring of intracellular cGMP. Nat Methods 3(1):23–25
131. Wallace DJ et al (2008) Single-spike detection in vitro and in vivo with a genetic Ca2+ sensor. Nat Methods 5(9):797–804
132. Shcherbo D et al (2009) Practical and reliable FRET/FLIM pair of fluorescent proteins. BMC Biotechnol 9:24
133. Zhang J et al (2001) Genetically encoded reporters of protein kinase A activity reveal impact of substrate tethering. Proc Natl Acad Sci U S A 98(26):14997–15002
134. Tsutsui H et al (2008) Improving membrane voltage measurements using FRET with new fluorescent proteins. Nat Methods 5(8):683–685
135. Mutoh H et al (2009) Spectrally-resolved response properties of the three most advanced FRET based fluorescent protein voltage probes. PLoS One 4(2):e4555
136. Tyas L et al (2000) Rapid caspase-3 activation during apoptosis revealed using fluorescence-resonance energy transfer. EMBO Rep 1(3):266–270
137. Wu X et al (2006) Measurement of two caspase activities simultaneously in living cells by a novel dual FRET fluorescent indicator probe. Cytometry A 69(6):477–486
138. Bozza WP et al (2014) The use of a stably expressed FRET biosensor for determining the potency of cancer drugs. PLoS One 9(9):e107010
139. Kominami K et al (2012) In vivo imaging of hierarchical spatiotemporal activation of caspase-8 during apoptosis. PLoS One 7(11):e50218
140. Sipieter F et al (2014) Shining light on cell death processes – a novel biosensor for necroptosis, a newly described cell death program. Biotechnol J 9(2):224–240
141. Li M et al (2012) A high-throughput FRET-based assay for determination of Atg4 activity. Autophagy 8(3):401–412
142. Lu P et al (2011) Extracellular matrix degradation and remodeling in development and disease. Cold Spring Harb Perspect Biol 3(12):a005058
143. Eichorst JP, Clegg RM, Wang Y (2012) Red-shifted fluorescent proteins monitor enzymatic activity in live HT-1080 cells with fluorescence lifetime imaging microscopy (FLIM). J Microsc 248(1):77–89
144. Hou BH et al (2011) Optical sensors for monitoring dynamic changes of intracellular metabolite levels in mammalian cells. Nat Protoc 6(11):1818–1833
145. Gavet O, Pines J (2010) Progressive activation of CyclinB1-Cdk1 coordinates entry to mitosis. Dev Cell 18(4):533–543
146. Miura H, Matsuda M, Aoki K (2014) Development of a FRET biosensor with high specificity for Akt. Cell Struct Funct 39(1):9–20
147. Yoshizaki H et al (2007) Akt-PDK1 complex mediates epidermal growth factor-induced membrane protrusion through Ral activation. Mol Biol Cell 18(1):119–128
148. Seong J et al (2013) Distinct biophysical mechanisms of focal adhesion kinase mechanoactivation by different extracellular matrix proteins. Proc Natl Acad Sci U S A 110 (48):19372–19377

149. Wang Y et al (2005) Visualizing the mechanical activation of Src. Nature 434 (7036):1040–1045
150. Vevea JD et al (2013) Ratiometric biosensors that measure mitochondrial redox state and ATP in living yeast cells. J Vis Exp 77:50633
151. Fehr M et al (2003) In vivo imaging of the dynamics of glucose uptake in the cytosol of COS-7 cells by fluorescent nanosensors. J Biol Chem 278(21):19127–19133
152. San Martin A et al (2013) A genetically encoded FRET lactate sensor and its use to detect the Warburg effect in single cancer cells. PLoS One 8(2):e57712
153. Nagai T, Miyawaki A (2004) A high-throughput method for development of FRET-based indicators for proteolysis. Biochem Biophys Res Commun 319(1):72–77
154. Mizutani T et al (2010) A novel FRET-based biosensor for the measurement of BCR-ABL activity and its response to drugs in living cells. Clin Cancer Res 16(15):3964–3975
155. Nobis M et al (2013) Intravital FLIM-FRET imaging reveals dasatinib-induced spatial control of src in pancreatic cancer. Cancer Res 73(15):4674–4686
156. Randriamampita C et al (2008) A novel ZAP-70 dependent FRET based biosensor reveals kinase activity at both the immunological synapse and the antisynapse. PLoS One 3(1):e1521
157. Paster W et al (2009) Genetically encoded Forster resonance energy transfer sensors for the conformation of the Src family kinase Lck. J Immunol 182(4):2160–2167
158. Grashoff C et al (2010) Measuring mechanical tension across vinculin reveals regulation of focal adhesion dynamics. Nature 466(7303):263–266
159. Conway DE et al (2013) Fluid shear stress on endothelial cells modulates mechanical tension across VE-cadherin and PECAM-1. Curr Biol 23(11):1024–1030
160. Borghi N et al (2012) E-cadherin is under constitutive actomyosin-generated tension that is increased at cell-cell contacts upon externally applied stretch. Proc Natl Acad Sci U S A 109 (31):12568–12573
161. Potzkei J et al (2012) Real-time determination of intracellular oxygen in bacteria using a genetically encoded FRET-based biosensor. BMC Biol 10:28
162. Conway JR, Carragher NO, Timpson P (2014) Developments in preclinical cancer imaging: innovating the discovery of therapeutics. Nat Rev Cancer 14(5):314–328
163. Bernardini A et al (2015) Type I cell ROS kinetics under hypoxia in the intact mouse carotid body ex vivo: a FRET-based study. Am J Physiol Cell Physiol 308(1):C61–C67
164. Awaji T et al (2001) Novel green fluorescent protein-based ratiometric indicators for monitoring pH in defined intracellular microdomains. Biochem Biophys Res Commun 289 (2):457–462
165. Urra J et al (2008) A genetically encoded ratiometric sensor to measure extracellular pH in microdomains bounded by basolateral membranes of epithelial cells. Pflugers Arch 457 (1):233–242
166. Heydorn A et al (2006) Protein translocation assays: key tools for accessing new biological information with high-throughput microscopy. Methods Enzymol 414:513–530
167. Knauer SK et al (2005) Translocation biosensors to study signal-specific nucleo-cytoplasmic transport, protease activity and protein-protein interactions. Traffic 6(7):594–606
168. Fetz V, Stauber RH, Knauer SK (2018) Translocation biosensors-versatile tools to probe protein functions in living cells. Methods Mol Biol 1683:195–210
169. Dieguez-Hurtado R et al (2011) A Cre-reporter transgenic mouse expressing the far-red fluorescent protein Katushka. Genesis 49(1):36–45
170. Yamaguchi Y et al (2011) Live imaging of apoptosis in a novel transgenic mouse highlights its role in neural tube closure. J Cell Biol 195(6):1047–1060
171. Audet M et al (2010) Protein-protein interactions monitored in cells from transgenic mice using bioluminescence resonance energy transfer. FASEB J 24(8):2829–2838
172. Hoffman RM (2005) The multiple uses of fluorescent proteins to visualize cancer in vivo. Nat Rev Cancer 5(10):796–806
173. Hara M et al (2004) Imaging endoplasmic reticulum calcium with a fluorescent biosensor in transgenic mice. Am J Physiol Cell Physiol 287(4):C932–C938

174. Zhang J et al (2005) Insulin disrupts beta-adrenergic signalling to protein kinase A in adipocytes. Nature 437(7058):569–573
175. Sun F et al (2018) A genetically encoded fluorescent sensor enables rapid and specific detection of dopamine in flies, fish, and mice. Cell 174(2):481–496.e19
176. Portugues R et al (2014) Whole-brain activity maps reveal stereotyped, distributed networks for visuomotor behavior. Neuron 81(6):1328–1343
177. Livet J et al (2007) Transgenic strategies for combinatorial expression of fluorescent proteins in the nervous system. Nature 450(7166):56–62
178. Nobis M et al (2017) A RhoA-FRET biosensor mouse for intravital imaging in normal tissue homeostasis and disease contexts. Cell Rep 21(1):274–288
179. Heppert JK et al (2016) Comparative assessment of fluorescent proteins for in vivo imaging in an animal model system. Mol Biol Cell 27(22):3385–3394
180. Hirayama T et al (2012) Near-infrared fluorescent sensor for in vivo copper imaging in a murine Wilson disease model. Proc Natl Acad Sci U S A 109(7):2228–2233
181. Giloh H, Sedat JW (1982) Fluorescence microscopy: reduced photobleaching of rhodamine and fluorescein protein conjugates by n-propyl gallate. Science 217(4566):1252–1255
182. White J, Stelzer E (1999) Photobleaching GFP reveals protein dynamics inside live cells. Trends Cell Biol 9(2):61–65
183. Dixit R, Cyr R (2003) Cell damage and reactive oxygen species production induced by fluorescence microscopy: effect on mitosis and guidelines for non-invasive fluorescence microscopy. Plant J 36(2):280–290
184. Niswender KD et al (1995) Quantitative imaging of green fluorescent protein in cultured cells: comparison of microscopic techniques, use in fusion proteins and detection limits. J Microsc 180(Pt 2):109–116
185. Shaner NC, Steinbach PA, Tsien RY (2005) A guide to choosing fluorescent proteins. Nat Methods 2(12):905–909
186. Shcherbakova DM, Verkhusha VV (2013) Near-infrared fluorescent proteins for multicolor in vivo imaging. Nat Methods 10(8):751–754
187. Nishihara R et al (2019) Highly bright and stable NIR-BRET with blue-shifted coelenterazine derivatives for deep-tissue imaging of molecular events in vivo. Theranostics 9(9):2646–2661